Molecular Basis of SARS-CoV-2 Nsp1-induced Immune Translational Shutdown as Revealed by All-Atom Simulations

Jure Borišek[‡], Angelo Spinello[†], Alessandra Magistrato*[,†]

‡National Institute of Chemistry, Hajdrihova 19, 1001 Ljubljana, Slovenia

†CNR-IOM-Democritos national Simulation Center c/o SISSA, Via Bonomea 265, 34136 Trieste, Italy

*Correspondence to alessandra.magistrato@sissa.it

Abstract

The severe acute respiratory syndrome coronavirus 2 (SARS-CoV-2) pandemic represents the most severe global health crisis in modern human history. One of the major SARS-CoV-2 virulence factors is nonstructural protein 1 (Nsp1), which, outcompeting with the binding of host messenger RNA (mRNA) to the human ribosome, triggers a translation shutdown of the host immune system. Here, microsecond-long all-atom simulations of the C-terminal portion of the SARS-CoV-2/SARS-CoV Nsp1 in complex with the 40S ribosome disclose that SARS-CoV-2 Nsp1 has evolved from its SARS-CoV ortholog to more effectively hijack the ribosome by undergoing a critical switch of Q/E158 and E/Q159 residues that perfects Nsp1's interactions with the ribosome. Our outcomes offer a basis for understanding the sophisticated mechanisms underlying SARS-CoV-2 diversion and exploitation of human cells components to its deadly purposes.

TOC Graphics

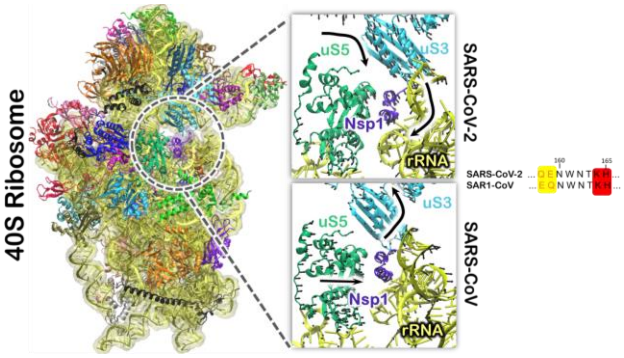

Coronaviruses normally cause mild respiratory infections (i.e. the common colds) in humans, albeit three highly pathogenic β-coronaviruses (β-CoVs) emerged in the last decades: Severe acute respiratory syndrome (SARS-CoV), Middle East respiratory syndrome (MERS-CoV), and Severe acute respiratory syndrome 2 (SARS-CoV-2). The latter, being causative agent of the ongoing COVID-19 pandemic, is hallmarked by a higher spread rate and a longer incubation period as compared to previous variants. Due to these noxious traits COVID-19 has rapidly become a major threat to human health, causing over 200 million cases and claiming almost 5 million lives by October 2021.[1]

In the last 1.5 years, the scientific community has undertaken a major research effort to decipher the molecular mechanisms underlying SARS-CoV-2 infection and to repurpose/develop antiviral drugs and/or vaccines and monoclonal antibodies to block/alleviate the COVID-19 disease.[2] Most studies have focused on the Spike glycoprotein,[3-6] which mediates the initial steps of SARS-CoV-2 infection.[7] Besides the infection, COVID-19 also elicits severe comorbid conditions, which affect disease progression and mortality in patients of all ages. The Nonstructural Protein 1 (Nsp1) is considered as one of the main comorbidity-inducing factors of COVID-19.[8-9] Nsp1 is indeed

one of the first proteins to be translated in infected cells and provokes a severe viability reduction in cells of lung origin by inducing a nearly complete shutdown of the cell's host gene expression. This inhibits all cellular antiviral defense mechanisms that rely on the expressions of host factors, including the interferon response. As such, Nsp1 contributes to suppress the host innate immune system and facilitate viral replication via distinct mechanisms:[10] (i) its C-terminal portion (C-term) binds to the messenger (m)RNA entry-tunnel of the human ribosome, triggering a significant translational reduction of host mRNA. Intriguingly, viral mRNA overcomes Nsp1-induced ribosome inhibition by an unclear mechanism.[11-12] (ii) The globular domain of Nsp1 recruits proteins to degrade mRNA strands that lack a viral tag (i.e. Nsp1 exclusively degrades human mRNA).[13-14] (iii) Finally, Nsp1 jams the exit channel of the nucleus to prevent the host mRNAs exit to the cytosol, where translation occurs.[15]

Regarding the first mechanism, a recent Cryo-EM structure trapped the C-term of SARS-CoV-2 Nsp1 in complex with the human ribosome.[8] This structure revealed that Nsp1 binds to the 40S ribosomal subunit within the mRNA entry-tunnel, which is lined by the uS3 and uS5 proteins and helix 18 (h18) of ribosomal RNA (rRNA). The C-term of Nsp1, folded into two α helices connected by a short loop, share 84% sequence identity with the SARS-CoV variant, arguing for functional orthology. Among the conserved residues, K164 and H165 are critical for translational shutdown, as their mutations to alanine was demonstrated to abolish Nsp1 binding to the ribosome.[8]

In vitro binding and translation assays also revealed that Nsp1 of both SARS-CoV and SARS-CoV-2 exerts similar efficacy and host translational shutdown mechanism.[8] Nevertheless, SARS-

CoV-2 is more infectious and triggers more comorbid conditions than SARS-CoV.[16] Aiming at unraveling how Nsp1 contributes to trigger a COVID-19-related burden, we elucidated the molecular subtleties of SARS-CoV/-2 Nsp1 binding to the 40S ribosome by performing all-atom molecular dynamics (MD) simulations.

Based on the recent cryo-EM structure of SARS-CoV-2 Nsp1 in complex with the 40S ribosome (PDB ID: 6ZLW),[8] we built a model system encompassing 34 proteins (all proteins of the 40S ribosome solved in the cryo-EM structure and the Nsp1 one), the rRNA, 29 Mg^{2+} and 3 Zn^{2+} ions, hereafter referred to as **SARS2** (Figure 1), which, upon explicit water solvation, counted 1,268,027 atoms.

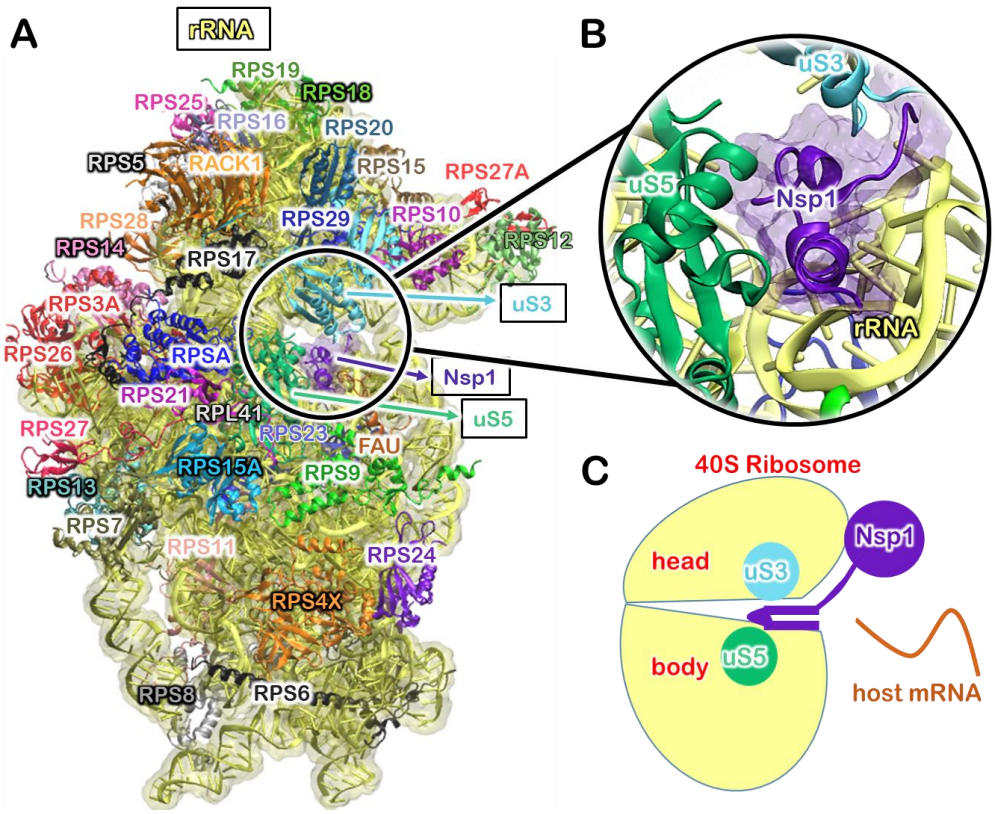

Figure 1. (A) Model of 40S ribosomal subunit in complex with the SARS-CoV-2 nonstructural protein 1 (Nsp1) built on cryo-EM structure (PDB ID: 6ZLW). Proteins and rRNA are depicted as new-cartoons. The names of the proteins of the Nsp1 binding tunnel are highlighted by black squares. (B) Inset of the Nsp1 binding site with Nsp1, uS3, uS5 proteins and ribosomal RNA shown in violet, cyan, green and yellow cartoons, respectively. (C) Schematic representation of Nsp1 binding to the 40S ribosome entry-tunnel located between the uS3 and uS5 proteins at the head and body of the 40S ribosome, respectively, showing hindering of host mRNA binding.

Next, we built a model system containing SARS-CoV Nsp1, hereafter referred to as **SARS1**. Since the C-term Nsp1 of the two SARS-CoV variants differs by eight amino acids, we introduced eight mutations into the Nsp1 protein of the previous model system. Conversely, for the apo ribosome, used as the reference structure, was generated by removing Nsp1 from the **SARS2** model (hereafter referred to as **APO)**. Each system underwent 1 μs-long all-atom MD simulation (MovieS1) (see Methods section in the Supporting Information (SI) for details).

Detailed inspection of the MD trajectories unraveled that Nsp1 has a similar, yet unevenly distributed, pattern of hydrogen (H)-bonds in the **SARS2** and **SARS1** orthologs (Figure 2, Table S1).

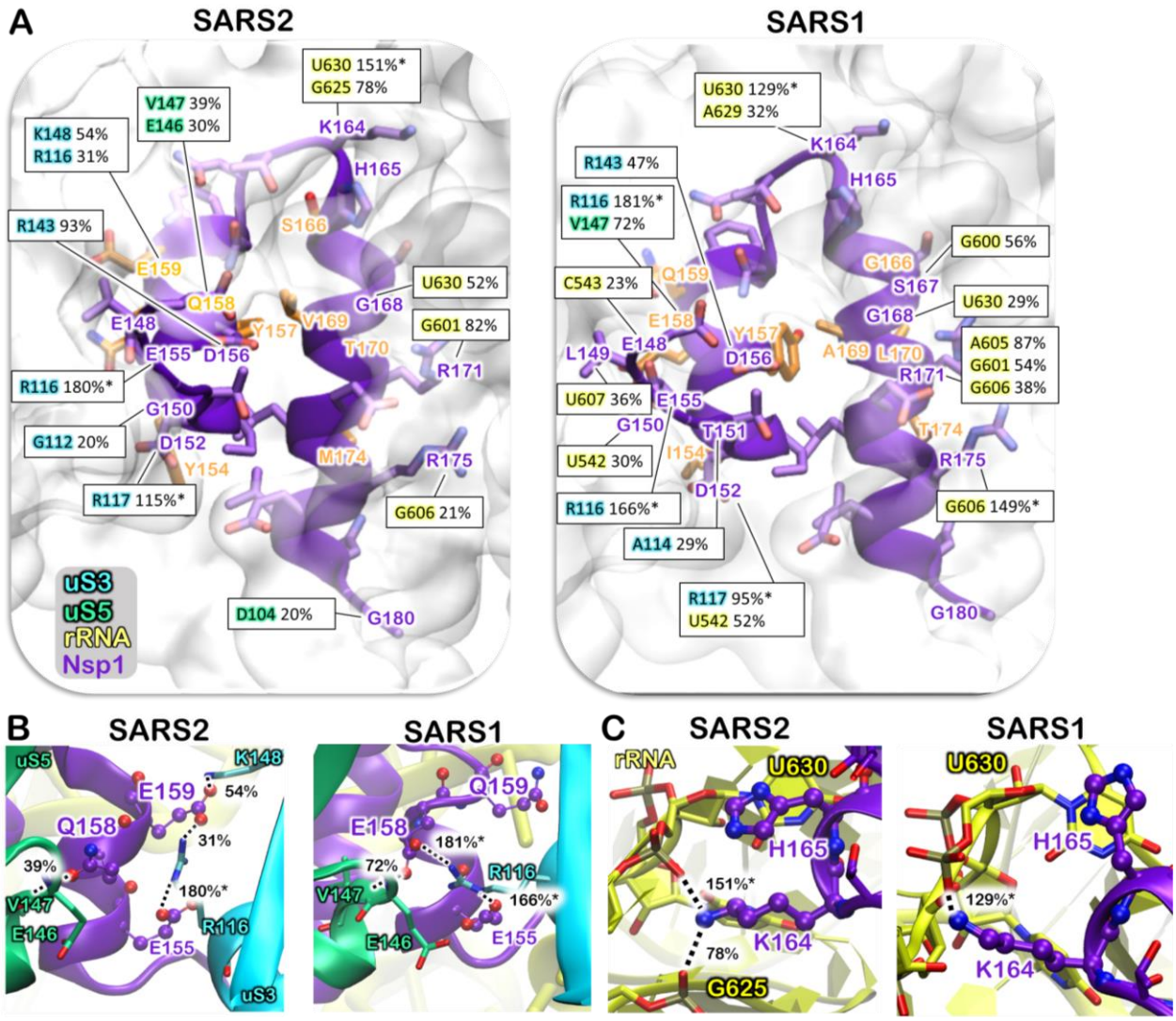

Figure 2. Representation of hydrogen (H)-bonding interactions of nonstructural protein 1 (Nsp1; violet) with ribosomal rRNA (yellow), and proteins uS3 (cyan), and uS5 (green) for **SARS2** and **SARS1** models. (A) Persistency of H-bond interactions of Nsp1 with the ribosome. For the residues displaying more than one H-bond moiety, the sum of their H-bond persistency is reported. The Nsp1 residues differing in the SARS-CoV and SARS-CoV-2 are colored in orange. (B) Magnified local interactions of mutated Q/E158 and E/Q159 SARS-CoV-2/SARS-CoV Nsp1 residues (presented with balls and sticks with reported H-bond persistency) with the surrounding uS5 and uS3 protein residues (shown as licorice). (C) Conserved K164 and H165 residues as

derived from the most representative cluster of molecular dynamics trajectories. H-bonds are indicated with dashed lines.

Noticeably, among the residues diverging in the two viral strains, is intriguing the switch of the glutamine and glutamate residues at position 158/159. These residues (Q/E158 and E/Q159 in **SARS2/SARS1**) link Nsp1 to the neighboring uS5 and uS3 proteins, and are strictly conserved only in the Nsp1 proteins of those β-CoV viral strains, which have been demonstrated to bind the human ribosome (Figure S1).[9]

A close inspection of their interaction patterns discloses that in **SARS1** E158 persistently salt-bridges to R116@uS3 (Figures 2A, B) and H-bonds to the V147@uS5 backbone, Q159 instead lacks any persistent contact with the nearby proteins or rRNA. Additionally, E155@Nsp1 lies in the vicinity of E146@uS5 (average distance of their Cδ atoms = 6.4 ± 0.4 Å), thus exerting an electrostatic repulsion, which weakens the interaction between Nsp1 and uS5. Conversely, in **SARS2** the swap between the Q/E158 and E/Q159 residues enables E159 to salt-bridge to R116@uS3 and K148@uS3, while Q158 H-bonds to the V147@uS5 backbone and the E146@uS5 side-chain, thus better mediating the connection between the body (uS5) and the head (uS3) of the 40S ribosome. In addition, the switch from E158 to Q158 in **SARS2** reduces the electrostatic repulsion with the nearby E146@uS5 residue. As a result of this interaction pattern remodeling, in **SARS2** even the key anchoring K164 and H165 residues better clasp Nsp1 at the bottom of the ribosome entry-tunnel with (i) K164, strongly interacting with the rRNA backbone phosphates G625 and U630, and (ii) H165 H-bonding with the U630 phosphate and π-stacking to the U630 base. Conversely, in **SARS1**, K164 only H-bonds to G625 phosphate, while H165 π-stacks with

U630 without establishing any H-bond interactions (Figure 2C). The effective interaction pattern established in SARS2 contributes to more rigidly trap Nsp1 within the ribosome, as revealed by its lower flexibility (Figure S2).

In line with the interactions discussed above, accessory energetic analyses disclose that in **SARS2** Nsp1 residues K164, H165, and E155 interact more strongly with the ribosome (Figure S3) and, that more in general Nsp1 better interacts with the uS3 and uS5 proteins as compared to **SARS1** (Figure S4), albeit in SARS1 Nsp1 overall displays better interaction and binding free energies.[17] Moreover, only small differences in rearrangement of hydrophobic interactions of the two models are observed, with W161 of Nsp1 forming T-shaped π-stacking with F124 of the uS5 protein only in **SARS2** (Figure S5).

To assess how a stitching of C-term-Nsp1 to the mRNA entry-tunnel affects the functional motions of the ribosome, we explored the internal dynamics of the distinct Nsp1/40S ribosome complexes by building the cross-correlation matrices in their standard (Figure S6) and coarse versions (see Supporting Methods section of the SI).[18] The latter variant of the cross-correlation matrix reports the sum of the cross-correlation coefficients of each couple of protein/RNA component of the simulated systems. This makes clear at the first glimpse the relevant cross-correlation coupling occurring in the system.[19-20] As a result, intriguing differences in the correlation pattern of Nsp1 with the uS3 and uS5 proteins emerged. Indeed, while Nsp1 correlates positively with uS5 in both systems, in **SARS1/SARS2** it negatively/positively correlates with both uS3 and rRNA. Additionally, uS3 and uS5 are negatively/positively correlated in **SARS1/SARS2**, while their correlation pattern is not clearly defined in **APO** (Figure 3).

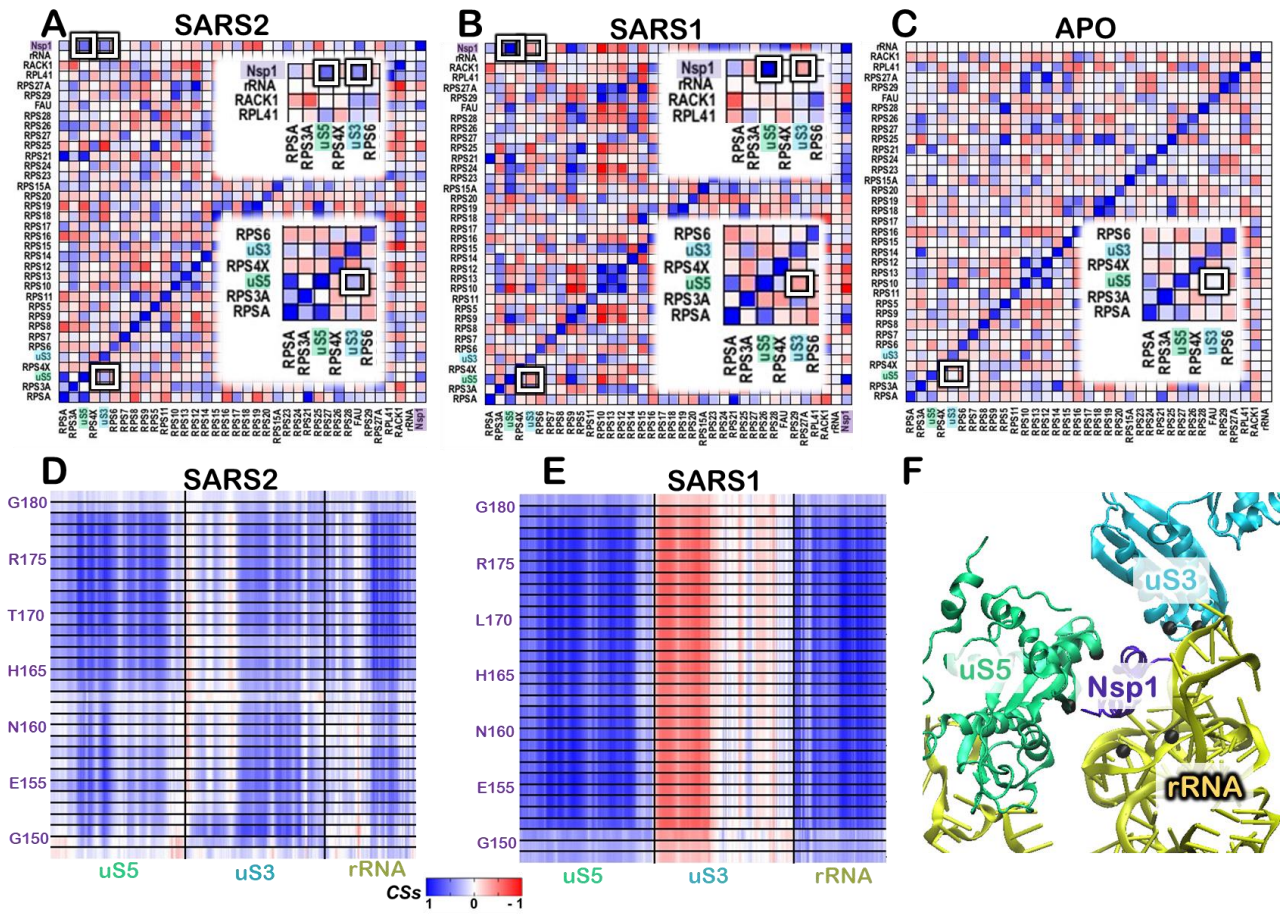

Figure 3. Cross-correlation matrix based on per-residue Pearson coefficients (*CCs*) as derived from the mass-weighted covariance matrix. CC values range from −1 (red, anticorrelated motions) to +1 (blue, correlated motions) and are accumulated for each pair of considered proteins/RNA and normalized to provide a density correlation score (*CS*). In white are encircled and magnified regions indicating the coupling of nonstructural protein 1 (Nsp1) binding pocket with the uS3 and uS5 proteins. Depicted are *CSs* of (A) **SARS2**, (B) **SARS1**, and (C) **APO** models. Submatrices of Nsp1 versus key residues of uS5, uS3 and rRNA lining the entry-tunnel for (D) **SARS2** and (E) **SARS1**. (F) View of the Nsp1 and the proteins lying the 40S ribosome entry-tunnel.

Next, in order to map how the distinct cross-correlation coupling may impact the large-scale collective motions of Nsp1/40S ribosome adducts, we performed the principal component analysis

of the MD trajectories[21] (Figures 4 and S7) focusing on the proteins and rRNA lining the mRNA entry-tunnel. Consistently with the cross-correlation maps detailed above, in **SARS2**, an effective twisting motion, adjuvated by the cooperation of the Nsp1, uS5 and uS3 proteins, induces a torque motion around Nsp1, thus triggering its closure of the ribosome entry-tunnel. This movement, possibly contributing to more effectively trap Nsp1 and to shutdown host mRNA translation, is absent in **SARS1** and **APO** (Figure 4 and Movies S2, S3 and S4).

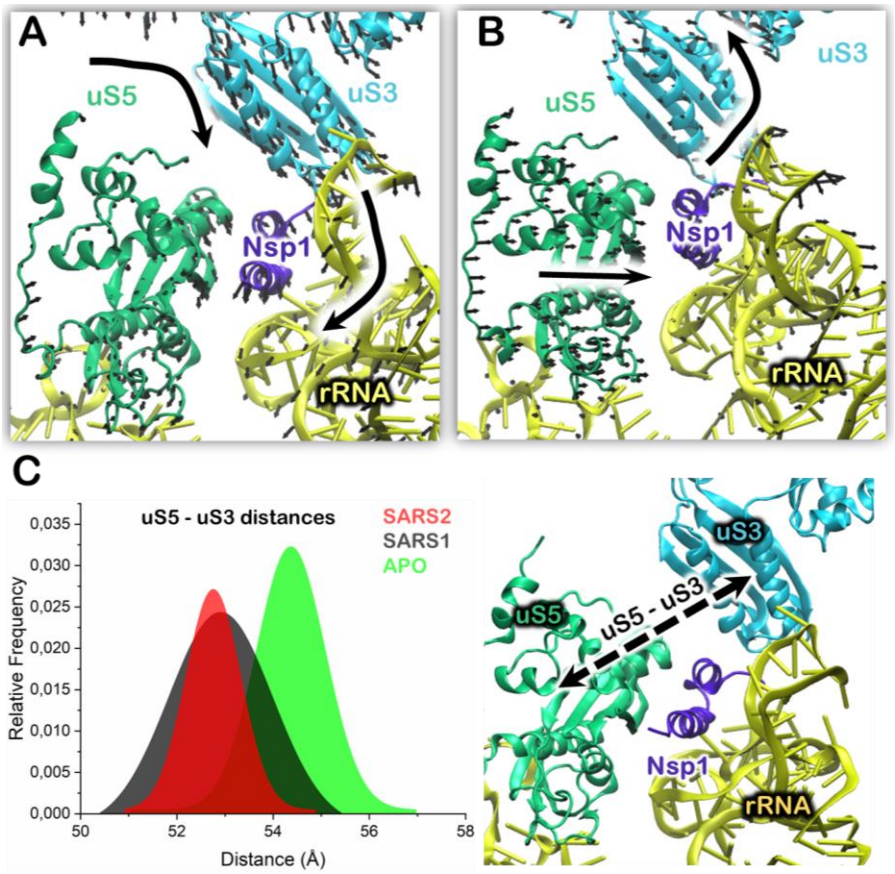

Figure 4. Essential dynamics as revealed by principal component analysis (PCA) (A) **SARS2** and (B) **SARS1**. The large black arrows highlight direction of the global motion of proteins/RNA lining the ribosome entry-tunnel. (C) Distribution of distances (Å) between the centers of mass of uS5 and uS3 proteins defining the width of the ribosome tunnel for **SARS2**, **SARS1** and **APO** models (depicted in red, black, and green, respectively) along the molecular dynamics trajectory.

In order to more quantitatively assess the impact of Nsp1 binding on tunnel width, we analyzed the distribution of the distance between the centers of mass of uS5 and uS3 proteins. This distance relates to the opening/closing motion of the ribosome head with respect to its body, where the uS3 and uS5 proteins belong, respectively. As a result, binding of Nsp1 from both viral strains closes the mRNA entry tunnel (Figures 4C), and shortening this distance, but the distribution is more peaked in **SARS2**, with a maximum lying at slightly smaller values, consistent with more effective entry-tunnel closure.

In summary, our outcomes expand current understanding of the SARS-CoV-2 mechanisms underlying invasion and diversion of human cells. Namely, by inspecting the atomic-level details of SARS-CoV/-2 Nsp1 binding to the 40S ribosome we revealed that in **SARS2** a critical switch of Q/E158 and E/Q159 residues remodels the interactions pattern between Nsp1 and the nearby proteins (uS3 and uS5) and rRNA (h18) lining the tunnel. This leads to better anchoring of Nsp1 at the bottom of the entry-tunnel and ultimately to a more effective tying of the ribosome head and body. In this scenario, it is tempting to argue that SARS-CoV-2 Nsp1 has evolved from its SARS-CoV ortholog to perfect selected key interactions with the ribosome in order to neatly stitch to and close the ribosome entry-tunnel and to more effectively suppress host translational shutdown, thus better exploiting human cells for its opportunistic and deadly objectives. This knowledge may be harnessed in future drug-discovery efforts aimed at reliving the COVID-19-related burden.

Supporting Information

The Supporting Information is available free of charge at https://pubs.acs.org/. Computational details, Tables S1, Figures S1 to S7, and Movies S1-S4.

Corresponding Author

Alessandra Magistrato - CNR-IOM c/o SISSA, via Bonomea 265, 34136 Trieste, Italy; http://orcid.org/0000-0002-2003-1985; Email: alessandra.magistrato@sissa.it

Authors

Jure Borišek - National Institute of Chemistry, Hajdrihova 19, 1001 Ljubljana, Slovenia; https://orcid.org/0000-0003-3417-0940

Angelo Spinello - CNR-IOM c/o SISSA, via Bonomea 265, 34136 Trieste, Italy; http://orcid.org/0000-0002-8387-8956

Notes

The authors declare no competing financial interest.

Acknowledgment

J.B. thanks Slovenian Research Agency (P1-0017 and Z1-1855) and A.M. thanks Italian Association for Cancer Research (IG. 24514) and of the project ARES CUP: D93D19000020007 POR FESR 2014 2020 - 1.3.b - Friuli Venezia Giulia for financial support. A.S. was supported by a FIRC-AIRC “Mario e Valeria Rindi” fellowship. The authors thank CINECA, the Italian supercomputing center, for computational resources via the “IsB23_RiboCoV” grant.

References

(1) de Wit, E.; van Doremalen, N.; Falzarano, D.; Munster, V. J. SARS and MERS: recent insights into emerging coronaviruses. *Nat. Rev. Microbiol.* **2016**, *14*, 523-534.

(2) Muratov, E. N.; Amaro, R.; Andrade, C. H.; Brown, N.; Ekins, S.; Fourches, D.; Isayev, O.; Kozakov, D.; Medina-Franco, J. L.; Merz, K. M.; Oprea, T. I.; Poroikov, V.; Schneider, G.; Todd, M. H.; Varnek, A.; Winkler, D. A.; Zakharov, A. V.; Cherkasov, A.; Tropsha, A. A critical overview of computational approaches employed for COVID-19 drug discovery. *Chem. Soc. Rev.* **2021**, *50*, 9121-9151.

(3) Sztain, T.; Ahn, S.-H.; Bogetti, A. T.; Casalino, L.; Goldsmith, J. A.; Seitz, E.; McCool, R. S.; Kearns, F. L.; Acosta-Reyes, F.; Maji, S.; Mashayekhi, G.; McCammon, J. A.; Ourmazd, A.; Frank, J.; McLellan, J. S.; Chong, L. T.; Amaro, R. E. A glycan gate controls opening of the SARS-CoV-2 spike protein. *Nat. Chem.* **2021**, *13*, 963–968

(4) Spinello, A.; Saltalamacchia, A.; Magistrato, A. Is the Rigidity of SARS-CoV-2 Spike Receptor-Binding Motif the Hallmark for Its Enhanced Infectivity? Insights from All-Atom Simulations. *J. Phys. Chem. Lett.* **2020**, *11*, 4785-4790.

(5) Spinello, A.; Saltalamacchia, A.; Borišek, J.; Magistrato, A. Allosteric Cross-Talk among Spike's Receptor-Binding Domain Mutations of the SARS-CoV-2 South African Variant Triggers an Effective Hijacking of Human Cell Receptor. *J. Phys. Chem. Lett.* **2021**, *12*, 5987-5993.

(6) Serapian, S. A.; Marchetti, F.; Triveri, A.; Morra, G.; Meli, M.; Moroni, E.; Sautto, G. A.; Rasola, A.; Colombo, G. The Answer Lies in the Energy: How Simple Atomistic Molecular Dynamics Simulations May Hold the Key to Epitope Prediction on the Fully Glycosylated SARS-CoV-2 Spike Protein. *J. Phys. Chem. Lett.* **2020**, *11*, 8084-8093.

(7) Harvey, W. T.; Carabelli, A. M.; Jackson, B.; Gupta, R. K.; Thomson, E. C.; Harrison, E. M.; Ludden, C.; Reeve, R.; Rambaut, A.; Peacock, S. J.; Robertson, D. L.; Conso, C.-G. U. C.-U. SARS-CoV-2 variants, spike mutations and immune escape. *Nat. Rev. Microbiol.* **2021**, *19*, 409-424.

(8) Thoms, M.; Buschauer, R.; Ameismeier, M.; Koepke, L.; Denk, T.; Hirschenberger, M.; Kratzat, H.; Hayn, M.; Mackens-Kiani, T.; Cheng, J. D.; Straub, J. H.; Sturzel, C. M.; Frohlich, T.; Berninghausen, O.; Becker, T.; Kirchhoff, F.; Sparrer, K. M. J.; Beckmann, R. Structural basis for translational shutdown and immune evasion by the Nsp1 protein of SARS-CoV-2. *Science* **2020**, *369*, 1249-1255.

(9) Schubert, K.; Karousis, E. D.; Jomaa, A.; Scaiola, A.; Echeverria, B.; Gurzeler, L. A.; Leibundgut, M.; Thiel, V.; Muhlemann, O.; Ban, N. SARS-CoV-2 Nsp1 binds the ribosomal mRNA channel to inhibit translation. *Nat. Struct. Mol. Biol.* **2020**, *27*, 959-966.

(10) Yuan, S.; Peng, L.; Park, J. J.; Hu, Y. X.; Devarkar, S. C.; Dong, M. B.; Shen, Q.; Wu, S. P.; Chen, S. D.; Lomakin, I. B.; Xiong, Y. Nonstructural Protein 1 of SARS-CoV-2 Is a Potent Pathogenicity Factor Redirecting Host Protein Synthesis Machinery toward Viral RNA. *Mol. Cell* **2020**, *80*, 1055-1066.

(11) Lapointe, C. P.; Grosely, R.; Johnson, A. G.; Wang, J. F.; Fernandez, I. S.; Puglisi, J. D. Dynamic competition between SARS-CoV-2 NSP1 and mRNA on the human ribosome inhibits translation initiation. *Proc. Natl. Acad. Sci. U. S. A.* **2021**, *118*, e2017715118.

(12) Simeoni, M.; Cavinato, T.; Rodriguez, D.; Gatfield, D. I(nsp1)ecting SARS-CoV-2–ribosome interactions. *Commun. Biol.* **2021**, *4*, 715.

(13) Finkel, Y.; Gluck, A.; Nachshon, A.; Winkler, R.; Fisher, T.; Rozman, B.; Mizrahi, O.; Lubelsky, Y.; Zuckerman, B.; Slobodin, B.; Yahalom-Ronen, Y.; Tamir, H.; Ulitsky, I.;

Israely, T.; Paran, N.; Schwartz, M.; Stern-Ginossar, N. SARS-CoV-2 uses a multipronged strategy to impede host protein synthesis. *Nature* **2021**, *594*, 240-245.

(14) Scudellari, M. How the coronavirus infects cells - and why Delta is so dangerous. *Nature* **2021**, *595*, 640-644.

(15) Zhang, K.; Miorin, L.; Makio, T.; Dehghan, I.; Gao, S. Y.; Xie, Y. H.; Zhong, H. L.; Esparza, M.; Kehrer, T.; Kumar, A.; Hobman, T. C.; Ptak, C.; Gao, B. N.; Minna, J. D.; Chen, Z. J.; Garcia-Sastre, A.; Ren, Y.; Wozniak, R. W.; Fontoura, B. M. A. Nsp1 protein of SARS-CoV-2 disrupts the mRNA export machinery to inhibit host gene expression. *Sci. Adv.* **2021**, *7*.

(16) Paules, C. I.; Marston, H. D.; Fauci, A. S. Coronavirus Infections-More Than Just the Common Cold. *JAMA* **2020**, *323*, 707-708.

(17) Genheden, S.; Ryde, U. The MM/PBSA and MM/GBSA methods to estimate ligand-binding affinities. *Expert Opin. Drug Discovery* **2015**, *10*, 449-461.

(18) Borišek, J.; Saltalamacchia, A.; Galli, A.; Palermo, G.; Molteni, E.; Malcovati, L.; Magistrato, A. Disclosing the Impact of Carcinogenic SF3b Mutations on Pre-mRNA Recognition Via All-Atom Simulations. *Biomolecules* **2019**, *9*, 633.

(19) Borišek, J.; Saltalamacchia, A.; Spinello, A.; Magistrato, A. Exploiting Cryo-EM Structural Information and All-Atom Simulations To Decrypt the Molecular Mechanism of Splicing Modulators. *J. Chem. Inf. Model.* **2020**, *60*, 2510–2521.

(20) Saltalamacchia, A.; Casalino, L.; Borišek, J.; Batista, V. S.; Rivalta, I.; Magistrato, A. Decrypting the Information Exchange Pathways across the Spliceosome Machinery. *J. Am. Chem. Soc.* **2020**, *142*, 8403–8411.

(21) David, C. C.; Jacobs, D. J. Principal Component Analysis: A Method for Determining the Essential Dynamics of Proteins. *Methods Mol. Biol.* **2014**, *1084*, 193-226.